Available online at www.sciencedirect.com
ScienceDirect
ELSEVIER
Photonics and Nanostructures – Fundamentals and Applications 5 (2007) 189–199
PHOTONICS AND NANOSTRUCTURES Fundamentals and Applications
www.elsevier.com/locate/photonics

The local density of states in finite size photonic structures, small particles approach

V. Prosentsov [a,*], A. Lagendijk [a,b]

[a] *Complex PhotonicSystems (COPS), Faculty of Science and Technology, and MESA+ Research Institute, University of Twente, P.O. Box 217, 7500 AE Enschede, The Netherlands*

[b] *FOM-Institute for Atomic and Molecular Physics, Kruislaan 407, 1098 SJ Amsterdam, The Netherlands*

Received 11 August 2006; received in revised form 25 July 2007; accepted 30 July 2007
Available online 8 August 2007

Abstract

The local density of states is studied with the help of the local perturbation method for vector and scalar wave fields propagating in finite size photonic structures. The local density of states is numerically calculated for one-, two-, and three-dimensional finite size photonic structures considering them as made of small particles.

PACS : 42.25.Bs; 42.25.Fx; 42.70.Qs

Keywords: Local density of states; Photonic crystal; Small particles

1. Introduction

The interaction of light with a medium belongs to the fundamental problems in physics. Recently it was found that systems with a periodic distribution of the index of refraction (photonic crystals) have many interesting properties, not only for pure science but also for practical applications (see for example book [1] and references therein). The quest for photonic crystals with prescribed properties has begun several years ago. The first commercial applications are the photonic crystal fibers with unusual dispersion and high numerical aperture. The fibers can be used as effective sources with broad spectrum and as high-power fiber lasers [2,3]. According to Ref. [4] a cluster of products based on photonic crystals will be available in near future, among them: photonic integrated circuits, antennas, and lasers. To use photonic crystals as lasers, control over enhancement and inhibition of light emission inside them will be crucial to improve laser efficiency. Recent experiments [5] show that the spectral distribution and the decay of light emitted from excitons confined in the quantum dots are controlled by the host photonic crystal.

Since the late nineteen forties it is well known that the spontaneous emission rate of an atom is not a constant, but a function of the atom's surrounding. [6] Fermi's golden rule states that the emission rate is proportional to the local density of states (LDOS) in a medium [7]. In addition, there can be a local field correction [8]. When the LDOS sharply variates as a function of frequency or position in the unit cell, the Wigner–Weisskopf approximation [9] breaks down and novel phenomena occur. Among which are non-Markovian behavior and nonexponential spontaneous emission accompanied by the change of the spectrum from a single Lorentzian peak into a two-peaked structure [10,11].

* Corresponding author. Tel.: +31 63 8233313.
E-mail address: prosentsov@yahoo.com (V. Prosentsov).

1569-4410/$ – see front matter © 2007 Elsevier B.V. All rights reserved.
doi:10.1016/j.photonics.2007.07.012

The most dramatic variations in the LDOS (and consequently in the spontaneous emission rate of an atom) were theoretically found in infinite photonic crystals having a full band gap [12–14]. In a band gap the LDOS drops to zero. In real photonic structures (which are always of finite size) there will be no complete band gap. However, the LDOS can still be small and strongly varying in space and frequency. The LDOS is directly related to the Green's function and depends on the spatial distribution of obstacles in a diffraction or scattering medium.

Due to the complex structure of photonic media, the theoretical study of the Green's functions is often limited to simplistic model systems and the impact of the local field effect has not even been considered up to now. For realistic structures numerical calculations are necessary. At first, the LDOS was studied in infinite photonic crystals (see for example Refs. [15–17] and references therein). These calculations, however, did not relate to the realistic photonic structures having for instance boundaries and defects. The study of the LDOS in the finite photonic crystals started several years ago and a number of interesting structures was considered. The LDOS for one-dimensional crystals was treated in Refs. [18,19]. In Refs. [20,21] the LDOS for the two-dimensional structures, consisting of cylinders, were calculated with the help of rigorous theory [22]. The LDOS was computed for the three-dimensional case with infinitely small plane scatterers [23] or cylinders [24] as the building blocks. In Refs. [25,26] the LDOS was studied in structures made out of particles (such as opals or inverse opals, for example) by using the finite difference (FD) methods. Such calculations however, require a lot of programming efforts, from one side, and sophisticated computers, from another side. In the FD methods an extremely large number of the grid points growing cubically with decreasing of mesh size, is needed. Moreover, the grid points should cover a free space between particles and voids inside a complex structure. The FD methods works usually in time domain and can not take directly dispersion into account. The dispersion can be handled via specially designed auxiliary differential equations [27,28]. Note that nonlinear effects and resonances can be also taken into account, however it will require even more computer resources.

Theoretically, each finite-sized photonic crystal can be treated as a structure made of a number of small (compared to the incident wavelength) particles. In this view one can consider the problem as a many particle scattering problem. As was shown in Refs. [29,30], the scattering from many small particles can be effectively treated in a pure numerical way with the help of the coupled dipole method. The modification of this method was used in Ref. [31] for numerical calculations of the density of states in arbitrary finite-size photonic structures. This method works in frequency domain and unlike the FD methods, requires field calculation only inside the scatterer.

Recently [32], resonance wave scattering by small particles of arbitrary shape was treated with the help of the local perturbation method [33–35]. The method is generalization of the coupled dipole approximation: it takes into account the shape of the particles and accurately reproduces the first scattering resonance. In contrast to the coupled dipole approximation, the local perturbation method allows to calculate fields in three-dimensional media with one- and two-dimensional periodicity. Below we will apply this method to the calculation of the LDOS in infinite and finite-size periodic structures. The method provides an effective and accurate way for numerical calculations of the LDOS in finite one-, two-, and three-dimensional photonic crystals and other structures made of small particles.

2. The LDOS in media with particles: vector waves

2.1. General considerations

The local density of states ρ in a dielectric medium is proportional to the imaginary part of the trace of the Green's tensor in polarization space and defined by the following expression (see, for example Ref. [23] and the interesting discussions therein about the definition of the LDOS)

$$\rho(\mathbf{r},\omega) = -\frac{2\omega\varepsilon_0}{\pi c^2}\,\mathrm{Im}[\mathrm{Tr}\hat{G}(\mathbf{r},\mathbf{r})], \tag{1}$$

where ω is the circular frequency, c the velocity of light in vacuum, ε_0 the permittivity of the host medium, and $\hat{G}(\mathbf{r},\mathbf{r}')$ is the Green's tensor at observation point $\mathbf{r}$ with source placed at point $\mathbf{r}'$. Im and Tr denote imaginary part and trace, respectively. Note that formula (1) holds in any dielectric medium without gain. In gain media the Green's tensor can be also calculated, however the LDOS in this case is not well defined. Expression (1) shows that the LDOS can be easily computed when the Green's tensor $\hat{G}(\mathbf{r},\mathbf{r}')$ is known. In the following we will calculate the Green's tensor with the help of the local perturbation method.

The equation for the Green's tensor in the medium has the form

$$\triangle\hat{G}(\mathbf{r},\mathbf{r}') - \nabla\otimes\nabla\hat{G}(\mathbf{r},\mathbf{r}') + \frac{\omega^2}{c^2}\varepsilon(\mathbf{r})\hat{G}(\mathbf{r},\mathbf{r}') = \hat{I}\delta(\mathbf{r}-\mathbf{r}'), \quad (2)$$

where $\otimes$ defines tensor product, $\varepsilon(\mathbf{r})$ the permittivity of the medium containing scatterers, $\hat{I}$ the 3×3 unitary tensor in polarization space, and δ is the Dirac delta function. The permittivity of the medium with N particles can be represented in the following form

$$\varepsilon(\mathbf{r}) = \varepsilon_0 + \sum_{n=1}^{N}(\varepsilon_n - \varepsilon_0) f_n(\mathbf{r}-\mathbf{r}_n), \quad (3)$$

where ε_n is the permittivity of the n th scatterer, and $f_n(\mathbf{r}-\mathbf{r}_n)$ is the unit step function describing the shape of the n th particle, such that

$$f_n(\mathbf{r}-\mathbf{r}_n) = \begin{cases} 1, & \text{inside particle} \\ 0, & \text{outside particle} \end{cases} \quad (4)$$

Taking into account formula (3) we rewrite the Eq. (2) for the Green's tensor in the following form

$$\triangle\hat{G}(\mathbf{r},\mathbf{r}') - \nabla\otimes\nabla\hat{G}(\mathbf{r},\mathbf{r}') + k_0^2\hat{G}(\mathbf{r},\mathbf{r}') + \frac{\omega^2}{c^2}\sum_{n=1}^{N}(\varepsilon_n - \varepsilon_0) f_n(\mathbf{r}-\mathbf{r}_n)\hat{G}(\mathbf{r},\mathbf{r}') = \hat{I}\delta(\mathbf{r}-\mathbf{r}'), \quad (5)$$

where $k_0 = \frac{\omega}{c}\sqrt{\varepsilon_0} = 2\pi/\lambda_0$ is the wave number in the host medium.

An approximate solution of the Eq. (5) can be found with the help of the local perturbation method [32] when characteristic size (L) of the scatterer is small compared to the incident wavelength, i.e. when $k_0L \ll 1$. The method is applied when the function $f_n(\mathbf{r}-\mathbf{r}_n)$ has a sharp maximum at some point (say, $\mathbf{r}_n$) and dies to zero in a finite (of a characteristic size L of the scatterer) vicinity of this point. It is interesting to note that there is no specific constraint on how fast the function $f_n(\mathbf{r}-\mathbf{r}_n)$ should decay with the distance. The key hypothesis of the local perturbation method is the assumption that the solution $\hat{G}(\mathbf{r},\mathbf{r}')$ is a relatively slow function of coordinates in this vicinity, so that

$$f_n(\mathbf{r}-\mathbf{r}_n)\hat{G}(\mathbf{r},\mathbf{r}') \approx f_n(\mathbf{r}-\mathbf{r}_n)\hat{G}(\mathbf{r}_n,\mathbf{r}'). \quad (6)$$

From the physical point of view this approximation means that the perturbation, being of an arbitrary strength, is concentrated in an area that is small compare to the wavelength λ_0 in surrounding media. Applying the LPM (6) we obtain from Eq. (5) that

$$\triangle\hat{G}(\mathbf{r},\mathbf{r}') - \nabla\otimes\nabla\hat{G}(\mathbf{r},\mathbf{r}') + k_0^2\hat{G}(\mathbf{r},\mathbf{r}') + \frac{\omega^2}{c^2}\sum_{n=1}^{N}(\varepsilon_n - \varepsilon_0) f_n(\mathbf{r}-\mathbf{r}_n)\hat{G}(\mathbf{r}_n,\mathbf{r}') = \hat{I}\delta(\mathbf{r}-\mathbf{r}'). \quad (7)$$

Eq. (7) can better be solved by using spatial Fourier transformation on the coordinate $\mathbf{r}$. The Fourier transform $\hat{G}(\mathbf{q},\mathbf{r}')$ of the Green's tensor takes the form

$$\hat{G}(\mathbf{q},\mathbf{r}') = \left(\hat{I} - \frac{\mathbf{q}\otimes\mathbf{q}}{k_0^2}\right)\left\{\frac{\mathrm{e}^{-i\mathbf{q}\cdot\mathbf{r}'}}{8\pi^3(k_0^2-q^2)} - \frac{\omega^2}{c^2}\sum_{n=1}^{N}(\varepsilon_n-\varepsilon_0)\hat{G}(\mathbf{r}_n,\mathbf{r}')\frac{f_n(\mathbf{q})\mathrm{e}^{-i\mathbf{q}\cdot\mathbf{r}_n}}{(k_0^2-q^2)}\right\}, \quad (8)$$

where

$$\hat{G}(\mathbf{q},\mathbf{r}') = \frac{1}{8\pi^3}\int_{-\infty}^{\infty}\int_{-\infty}^{\infty}\int_{-\infty}^{\infty}\hat{G}(\mathbf{r},\mathbf{r}')\mathrm{e}^{-i\mathbf{q}\cdot\mathbf{r}}\,\mathrm{d}\mathbf{r},$$
$$f_n(\mathbf{q})\mathrm{e}^{-i\mathbf{q}\cdot\mathbf{r}_n} = \frac{1}{8\pi^3}\int_{-\infty}^{\infty}\int_{-\infty}^{\infty}\int_{-\infty}^{\infty} f_n(\mathbf{r}-\mathbf{r}_n)\mathrm{e}^{-i\mathbf{q}\cdot\mathbf{r}}\,\mathrm{d}\mathbf{r}, \quad (9)$$

are the Fourier transforms of $\hat{G}(\mathbf{r},\mathbf{r}')$ and $f_n(\mathbf{r}-\mathbf{r}_n)$, respectively. Fourier transforming of (8) back to the real space gives

$$\hat{G}(\mathbf{r},\mathbf{r}') = \hat{G}_0(\mathbf{r},\mathbf{r}') - \frac{\omega^2}{c^2}\left(\hat{I} + \frac{\nabla\otimes\nabla}{k_0^2}\right) \times \sum_{n=1}^{N}(\varepsilon_n-\varepsilon_0)\hat{G}(\mathbf{r}_n,\mathbf{r}') \times \int_{-\infty}^{\infty}\int_{-\infty}^{\infty}\int_{-\infty}^{\infty}\frac{f_n(\mathbf{q})\mathrm{e}^{i\mathbf{q}\cdot(\mathbf{r}-\mathbf{r}_n)}}{(k_0^2-q^2)}\,\mathrm{d}\mathbf{q}, \quad (10)$$

where $\hat{G}_0(\mathbf{r},\mathbf{r}') = -\left(\hat{I} + \frac{\nabla\otimes\nabla}{k_0^2}\right)\frac{\mathrm{e}^{ik_0R}}{4\pi R}$ is the Green's tensor of free space and $R = |\mathbf{r}-\mathbf{r}'|$ is the distance between the observation point and the source.

Formula (10) is the main result of this section. It explicitly shows that the total Green's tensor is a sum of the free space term $\hat{G}_0$ and term due to the scattering by particles. The last one is proportional to the contrast of the particles $\varepsilon_n - \varepsilon_0$ and depends on the particle's shape f_n. The interaction between the scatterers and their resonance properties are taken into account by terms $\hat{G}(\mathbf{r}_n,\mathbf{r}')$ that should be found.

For spherically symmetric scatterers ($f_n(\mathbf{q}) = f_n(|\mathbf{q}|)$), the second integral in (10) can be explicitly calculated with the help of the of method of residues.

We obtain

$$\hat{G}(\mathbf{r},\mathbf{r}') = \hat{G}_0(\mathbf{r},\mathbf{r}') + 2\pi^2\frac{\omega^2}{c^2}\left(\hat{I}+\frac{\nabla\otimes\nabla}{k_0^2}\right) \times \sum_{n=1}^{N}(\varepsilon_n-\varepsilon_0)f_n(k_0)\hat{G}(\mathbf{r}_n,\mathbf{r}')\frac{e^{ik_0R_n}}{R_n}, \qquad (11)$$

where $R_n = |\mathbf{r}-\mathbf{r}_n|$ is the distance between the observation point and n th scatterer. Note that $f_n(k_0) \simeq V_n/8\pi^3$, where V_n is volume of the n th scatterer. Formula (11) gives the Green's tensor of a medium filled with N small spherically symmetric particles within local perturbation method. The formulas (10) and (11) contain unknown tensors $\{\hat{G}(\mathbf{r}_n,\mathbf{r}')\}$ which can be calculated by solving system of $9\times 9N$ linear equations obtained by substituting $\mathbf{r}$ by $\mathbf{r}_n$ into (10). More detailed calculation of the tensors $\{\hat{G}(\mathbf{r}_n,\mathbf{r}')\}$ is presented in Appendix A. Remarkably, result (11) can also be obtained also with the help of the theory of point scatterers involving momentum cut-off procedure and proper regularization of the Green's tensor [36].

In accordance with formula (1), the LDOS of the medium filled by spherically symmetric particles is

$$\rho(\mathbf{r},\omega) = \rho_0(\omega) - \frac{\omega^3\varepsilon_0}{2\pi^2c^4}\sum_{n=1}^{N}(\varepsilon_n-\varepsilon_0)\frac{V_n}{R_n} \times \mathrm{Im}\left[\mathrm{Tr}\hat{G}(\mathbf{r}_n,\mathbf{r})e^{ik_0R_n}\right], \qquad (12)$$

where $\rho_0(\omega) = \frac{\omega^2\varepsilon_0^{3/2}}{\pi^2c^3}$ is the LDOS of the homogeneous host medium with permittivity ε_0. Formula (12) explicitly shows that additional contribution in the LDOS is proportional to volume of the scatterer V_n and decreases with the distance R_n between n th particle and observer.

Scatterers can be placed randomly or periodically as in a photonic crystal. In the latter case formula (12) describes the LDOS in a photonic crystal formed by small particles. A defect in such structure is simply the presence or absence of one or more scatterers. Such a defect can be easily incorporated in our formalism.

It should be noted that, when the scatterer is not sufficiently small ($k_0L \geq 0.2$, for example), it should be subdivided into smaller particles with size L_{sub} such that $k_0L_{\mathrm{sub}} \leq 0.1$. Subdivision procedure and its properties will be discussed in detail in the following.

2.2. Numerical examples

2.2.1. The LDOS of the small sphere

It is worth to consider the Green's function and the LDOS when only one, for example, spherical particle is placed in the medium at point $\mathbf{r}_1$. In this case formula (11) for the Green's tensor (11) takes the following form

$$\hat{G}(\mathbf{r},\mathbf{r}') = \hat{G}_0(\mathbf{r},\mathbf{r}') + \frac{\omega^2V_1}{4\pi c^2}\left(\hat{I}+\frac{\nabla\otimes\nabla}{k_0^2}\right) \times (\varepsilon_1-\varepsilon_0)\hat{G}(\mathbf{r}_1,\mathbf{r}')\frac{e^{ik_0R_1}}{R_1}, \qquad (13)$$

where $\hat{G}(\mathbf{r}_1,\mathbf{r}')$ is the Green's tensor at point $\mathbf{r}_1$ where the particle is placed. The unknown tensor $\hat{G}(\mathbf{r}_1,\mathbf{r}')$ better be calculated with the help of formula (10) when $\mathbf{r} = \mathbf{r}_1$ (more details one can find in Appendix A). The expression for the tensor $\hat{G}(\mathbf{r}_1,\mathbf{r}')$ looks like

$$\hat{G}(\mathbf{r}_1,\mathbf{r}') = \frac{3\varepsilon_0\hat{G}_0(\mathbf{r}_1,\mathbf{r}')}{D(\omega,L)}, \qquad (14)$$

where

$$D(\omega,L) = 2\varepsilon_0+\varepsilon_1-(\varepsilon_1-\varepsilon_0)k_0^2L^2\left(1+2ik_0\frac{L}{3}\right). \qquad (15)$$

Here L is the characteristic size (radius) of the scatterer. It is interesting to note that formula (14) shows that there is scattering resonance at some wavelength. Our calculations show that this wavelength is predicted correctly, while the criterion $k_0L \ll 1$ is not satisfied in this spectral region. In accordance with formulas (1), (13), and (14) the LDOS for the small sphere is

$$\rho(\mathbf{r},\omega) = \rho_0(\omega) + \frac{3k_0^2V_1}{4\pi R_1}(\varepsilon_1-\varepsilon_0) \times \mathrm{Im}\left[\mathrm{Tr}\left(\hat{I}+\frac{\nabla\otimes\nabla}{k_0^2}\right)\frac{\hat{G}_0(\mathbf{r}_1,\mathbf{r}')}{D(\omega,L)}e^{ik_0R_1}\right]. \qquad (16)$$

It is interesting to compare our results with results predicted by the exact theory for the LDOS of a single sphere. For the calculation we choose the following realistic parameters: radius of the sphere is $L = 0.3\ \mu\mathrm{m}$, its permittivity is $\varepsilon_1 = 9$, and permittivity of the host medium is $\varepsilon_0 = 1$. Fig. 1 shows the LDOS calculated by using the exact Green's function for a sphere [37] and the LDOS given by formula (16) versus size parameter k_0L for different observation points outside of the particle. Fig. 1 explicitly shows that the results obtained by using our approximation agree extremely well with exact results for size parameters $k_0L \lesssim 0.2$. The agreement becomes even better with increasing of the distance between the particle and observation point.

2.2.2. The LDOS of a small cube

Another interesting example (having no exact solution as well) is the calculation of the LDOS for a small cube. By using the LPM the LDOS at the presence of the small cube can be studied analogically as it was

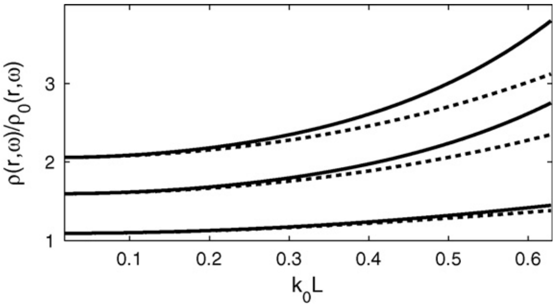

Fig. 1. The normalized LDOS of small sphere versus size parameter k_0L for different observation points. The parameters of the sphere are $L = 0.3\ \mu\text{m}$, $\varepsilon_1 = 9$, $\varepsilon_0 = 1$, and the observation points are $|\mathbf{r}| = L$ (two upper curves), $1.1L$ (two middle curves), and $1.5L$ (two lowest curves). The solid curves show exact results and the dashed ones represent our results.

done for the small sphere. The expression for the LDOS is the same as the expression (16) while the denominator D is changed to

$$D(\omega, L) = 2\varepsilon_0 + \varepsilon_1 - 1.32(\varepsilon_1 - \varepsilon_0)k_0^2L^2\left(1 + 3ik_0\frac{L}{\pi}\right). \tag{17}$$

Fig. 2 shows the LDOS calculated for the cube with size (half width) $L = 0.3\ \mu\text{m}$ and permittivity $\varepsilon_1 = 9$ placed in the host medium with permittivity $\varepsilon_0 = 1$. It should be noted that at this approximation the influence of edges or corners of a cube are not taken into account. Effectively, cube is treated as a sphere with slightly different radius. In order to see the influence of the features of the cube (even small one) one should subdivide the particle further on.

2.2.3. The LDOS of the cube and sphere

The LDOS of arbitrary structure made of N small spheres is given by formula (12). The LDOS of the array of particles (or single one) that are not small compare to the incident wavelength can be found by using subdivision preserving complete volume filling. Cubes are most suitable for such purpose: they have relatively simple shape and they can fill sphere, cube, or any other particle without voids. In this case general formula (10) should be applied. The only drawback in this case is that subdivision by cubes is not suitable very well for curved surfaces, and as result one should use a lot of subdivisions (i.e. cubes) substantially increasing by this the amount of computer's memory. Figs. 3 and 4 show for example the LDOS calculated for the cube and sphere, respectively for different number of subdivisions. The figures clearly show resonances and good convergence.

It should be noted here that all calculations were performed with the help of the 1.6 GHz personal computer on Matlab, running in Windows XP. The internal memory was sufficient only for 11 subdivisions (along each axis) of a sphere, that is 739 small cubes. For 150 frequency slots time of calculation was around 13 h.

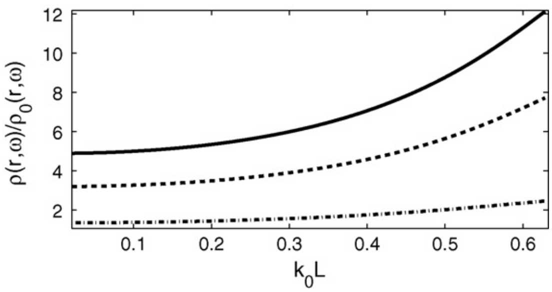

Fig. 2. The normalized LDOS of small cube versus size parameter k_0L for different observation points. The parameters of the cube are: $L = 0.3\ \mu\text{m}$, $\varepsilon_1 = 9$, $\varepsilon_0 = 1$, and observation points are $x = L$ (solid curve), $1.1L$ (dashed curve), $1.5L$ (dash-dotted curve), and $y = z = 0$.

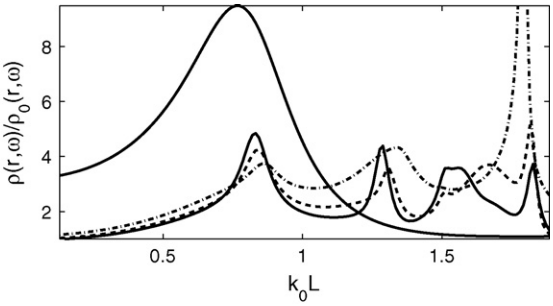

Fig. 3. The normalized LDOS of the cube versus size parameter k_0L for different subdivisions by cubes at the point $x = 1.1L$, $y = z = 0$. The parameters of the cube are $L = 0.3\ \mu\text{m}$, $\varepsilon_1 = 9$, and $\varepsilon_0 = 1$. The upper and the lower solid curves were calculated with 1 and 9 subdivisions along each spatial axis, the dash-dotted and the dashed curves were calculated with 5 and 7 subdivisions, respectively.

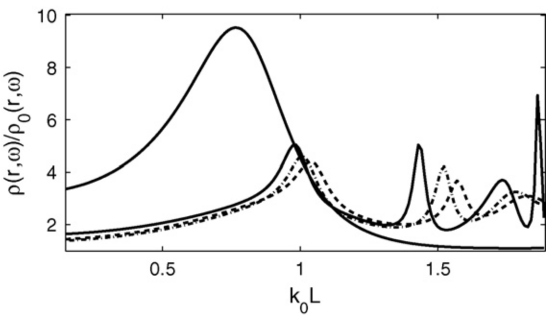

Fig. 4. The normalized LDOS of sphere versus size parameter k_0L for different subdivisions by cubes at the point $x = 1.1L$, $y = z = 0$. The parameters of the sphere are $L = 0.3\ \mu\text{m}$, $\varepsilon_1 = 9$, and $\varepsilon_0 = 1$. The upper solid curve was calculated with 1 subdivision and the lower solid curve is the exact result, the dash-dotted and the dashed curves were calculated with 9 and 11 subdivisions, respectively.

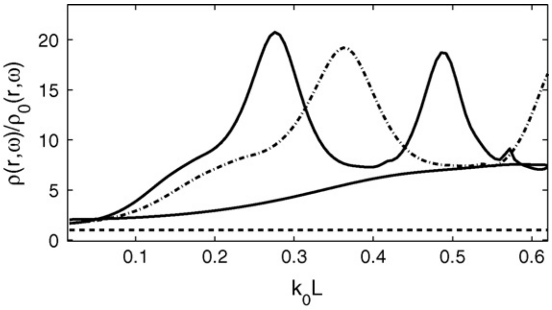

Fig. 5. The normalized LDOS of the cluster of spheres versus size parameter k_0L for different numbers of shells of the cluster at the point $x = L, y = z = 0$. The parameters of the spheres are $L = 0.3\,\mu$m, $\varepsilon_1 = 9$, and $\varepsilon_0 = 1$. The spheres are arranged into fcc lattice with filling fraction $\beta = 0.7$. The number of the shells of the cluster are 2, 4 and 5 (lower solid, dash-doted, and upper solid curves, respectively). The dashed line corresponds to the LDOS of free space.

2.2.4. The LDOS of cluster of small spheres

Fig. 5 shows the normalized LDOS calculated inside the cluster of small spheres (radius $L = 0.3\,\mu$m and permittivity $\varepsilon_n = 9$) placed in the host medium with $\varepsilon_0 = 1$. Figure explicitly shows oscillations in the LDOS due to the finite size of the cluster. With increasing the number of shells, the frequency of oscillations will grow.

3. The LDOS in media with particles: scalar waves

The scalar case is much easier compared to the vector one and it is less general. However, it still has some applications. Namely, wave phenomena associated with vector waves can be considered with the help of scalar technique for one-dimensional (1D) and two-dimensional (2D) structures when polarization of electric field is parallel to the direction where refractive index is constant.

Formally, the Green's tensor and the LDOS in scalar case are described by the same formulas as for vector one, excluding the depolarization term $\frac{\nabla\otimes\nabla}{k_0^2}$. As the result, the Green's tensor is replaced by the Green's function and expression for the LDOS in scalar case takes the form

$$\rho(\mathbf{r},\omega) = \rho_0(\omega) + \frac{2\omega^3\varepsilon_0}{\pi c^4}\sum_{n=1}^{N}(\varepsilon_n - \varepsilon_0) \times \mathrm{Im}\left[G(\mathbf{r}_n,\mathbf{r}')\int_{-\infty}^{\infty}\int_{-\infty}^{\infty}\int_{-\infty}^{\infty}\frac{\tilde{f}_n(\mathbf{q})\mathrm{e}^{i\mathbf{q}\cdot(\mathbf{r}-\mathbf{r}_n)}}{(k_0^2 - q^2)}\,\mathrm{d}\mathbf{q}\right], \tag{18}$$

where $\rho_0(\omega) = \frac{\omega^2\varepsilon_0^{3/2}}{2\pi^2c^3}$ is the scalar the LDOS of the homogeneous host medium.

3.1. The LDOS in 3D media with 1D and 2D scatterers

We consider the LDOS in the 3D media with 1D and 2D scatterers, i.e. infinite layers and cylinders, respectively. There are some peculiarities complicating the solution of the 1D–2D problem. We suppose that the layers are perpendicular to the x axis and the cylinders are oriented along the z axis. The general scheme for calculating the LDOS is the following: (1) obtain the expression for the Fourier transform of the Green's function $G(\mathbf{q},\mathbf{r}')$ in the form similar to expression (8) taking into account that for 1D and 2D scatterers we will need $f_n(x)$ and $f_n(\mathbf{r}_\perp(x,y))$, respectively; (2) integrate $G(\mathbf{q},\mathbf{r}')$ over q_x or $\mathbf{q}_\perp$ and obtain the expression for $G(x,\mathbf{q}_\perp,\mathbf{r}')$ or $G(\mathbf{r}_\perp,q_z,\mathbf{r}')$ for the 1D and 2D scatterers, respectively; (3) calculate the Green's functions $G(x,\mathbf{q}_\perp,\mathbf{r}')$ and $G(\mathbf{r}_\perp,q_z,\mathbf{r}')$ at points x_n and $\mathbf{r}_{\perp n}$, i.e. inside layers and cylinders, respectively; (4) integrate expressions for $G(x,\mathbf{q}_\perp,\mathbf{r}')$ and $G(\mathbf{r}_\perp,q_z,\mathbf{r}')$ over $\mathbf{q}_\perp$ and q_z, respectively.

3.1.1. 3D media with layers

Consider the LDOS in a 3D medium containing N scattering layers of thickness L. Following the scheme we obtain expression for the Green's function $G(\mathbf{q},\mathbf{r}')$ (compare to formula (8))

$$G(\mathbf{q},\mathbf{r}') = \frac{\mathrm{e}^{-i\mathbf{q}\cdot\mathbf{r}'}}{8\pi^3(k_0^2 - q^2)} - \frac{\omega^2}{c^2}\sum_{n=1}^{N}(\varepsilon_n - \varepsilon_0)f_n(q_x)G(x_n,\mathbf{q}_\perp,\mathbf{r}')\frac{\mathrm{e}^{-iq_xx_n}}{(k_0^2 - q^2)}, \tag{19}$$

where $f_n(q_x)$ is the 1D Fourier transform of the function $f_n(x)$ and $\mathbf{q}_\perp = \{q_y, q_z\}$. Note that the unknown functions $G(x_n,\mathbf{q}_\perp,r')$ are involved in formula (19). In order to find them we integrate expression (19) over q_x and obtain

$$G(x,\mathbf{q}_\perp,\mathbf{r}') = \frac{(-i)\mathrm{e}^{-i\mathbf{q}_\perp\cdot\mathbf{r}'_\perp + ik_{0x}|x-x'|}}{8\pi^2k_{0x}} + \pi i\frac{\omega^2}{c^2}\sum_{n=1}^{N}(\varepsilon_n - \varepsilon_0)f_n(k_{0x})G(x_n,\mathbf{q}_\perp,\mathbf{r}')\frac{\mathrm{e}^{ik_{0x}|x-x_n|}}{k_{0x}}, \tag{20}$$

where $k_{0x} = \sqrt{k_0^2 - q_\perp^2}$. The unknown functions $G(x_n,\mathbf{q}_\perp,r')$ are to be found from the set of equations obtained from formula (20) by substituting x by $\{x_n\}$. The last step is to integrate (20) over $\mathbf{q}_\perp$ that can be done only if explicit form of $G(x_n,\mathbf{q}_\perp,\mathbf{r}')$ is known.

The problem, however, can be solved in general by taking into account that solutions $G(x_n, \mathbf{q}_\perp, \mathbf{r}')$ can be presented in the following form

$$G(x_n, \mathbf{q}_\perp, \mathbf{r}') = \frac{g_n(k_{0x})}{D(k_{0x})} \mathrm{e}^{-i\mathbf{q}_\perp \cdot \mathbf{r}'_\perp}, \tag{21}$$

where $g_n(k_{0x})$ are functions depending on position x_n and k_{0x}, $D(k_{0x})$ is the determinant of the system of equations for $G(x_n, \mathbf{q}_\perp, \mathbf{r}')$. Substituting expression (21) into formula (20) and setting $\mathbf{r} = \mathbf{r}'$, and integrating over $\mathbf{q}_\perp$, we obtain for the LDOS

$$\rho(\mathbf{r}, \omega) = \rho_0(\omega) - 2\frac{\omega^3 \varepsilon_0}{c^4} \sum_{n=1}^{N} (\varepsilon_n - \varepsilon_0) \times \mathrm{Im}\left[i \int_{-\infty}^{\infty} \int_{-\infty}^{\infty} f_n(k_{0x}) \frac{g_n(k_{0x})}{D(k_{0x})} \frac{\mathrm{e}^{ik_{0x}|x-x_n|}}{k_{0x}} \mathrm{d}\mathbf{q}_\perp \right], \tag{22}$$

The integral in (22) is evaluated with the help of the residue theorem resulting in

$$\rho(\mathbf{r}, \omega) = \rho_0(\omega) + 8\pi^2 \frac{\omega^3 \varepsilon_0}{c^4} \sum_{n,m=1}^{N,M} (\varepsilon_n - \varepsilon_0) \times \mathrm{Im}\left[f_n(k_{0x}) \frac{g_n(k_{0x})}{(\mathrm{d}D(k_{0x}))/(\mathrm{d}q_\perp)} \frac{q_\perp \mathrm{e}^{ik_{0x}|x-x_n|}}{k_{0x}} \bigg|_{q_\perp = q_{\perp m}} \right]. \tag{23}$$

Here $(\mathrm{d}D(k_{0x}))/(\mathrm{d}q_\perp)$ is the derivative of the determinant D with respect to $q_\perp$, and $q_{\perp m}$ is the m th root of the equation $D(k_{0x}) = 0$. It is interesting to note here that $D(k_{0x}) = 0$ is the dispersion equation for all modes (propagating and evanescent) in the structure. Thus, formula (23) explicitly shows that the LDOS is affected by all modes existing in the structure.

3.1.2. 3D media with cylinders

The LDOS in the 3D media with cylinders can be treated in a similar manner as it was done for layers. The final expressions for the Green's function $G(\mathbf{r}_\perp, q_z, \mathbf{r}')$ and the LDOS are

$$G(\mathbf{r}_\perp, q_z, \mathbf{r}') = \frac{(-i)}{8\pi} H_0^{(1)}(k_{0\perp}|\mathbf{r}_\perp - \mathbf{r}'_\perp|)\mathrm{e}^{-iq_z z'} + \pi^2 i \frac{\omega^2}{c^2} \times \sum_{n=1}^{N} (\varepsilon_n - \varepsilon_0) f_n(k_{0\perp}) G(\mathbf{r}_{\perp n}, q_z, \mathbf{r}') \times H_0^{(1)}(k_{0\perp}|\mathbf{r}_\perp - \mathbf{r}_{\perp n}|), \tag{24}$$

$$\rho(\mathbf{r}, \omega) = \rho_0(\omega) + 4\pi^2 \frac{\omega^3 \varepsilon_0}{c^4} \sum_{n,m=1}^{N,M} (\varepsilon_n - \varepsilon_0) \times \mathrm{Im}\left[f_n(k_{0\perp}) \frac{g_n(k_{0\perp})}{(\mathrm{d}D(k_{0\perp}))/(\mathrm{d}q_z)} \times H_0^{(1)}(k_{0\perp}|\mathbf{r}_\perp - \mathbf{r}_{\perp n}|) \bigg|_{q_z = q_{zm}} \right]. \tag{25}$$

Here $H_0^{(1)}$ is the Hankel function of the first kind and zeroth order, $k_{0\perp} = \sqrt{k_0^2 - q_z^2}$, $f_n(k_{0\perp})$ is the 2D Fourier transform of the function $f_n(\mathbf{r}_\perp)$, and q_{zm} is the m th root of the dispersion equation $D(k_{0\perp}) = 0$.

3.2. The LDOS in 1D and 2D media

Notwithstanding the fact that real photonic crystals are 3D structures and the LDOS in 3D media in general is not related to the LDOS in lower dimensional media, there are several benefits for considering 1–2D media. Firstly, one can relatively easy calculate and compare the LDOS obtained with different methods. Secondly, the Green's function obtained for the LDOS can be used for calculation of transmission coefficient for structures in 1D media.

The LDOS in 1D and 2D media can be calculated in the same manner as it was done for the 3D media. We present only the final results. The Green's function in the 1D case is given by

$$G(x, x') = G_0(x, x') + \frac{i\omega}{2c\sqrt{\varepsilon_0}} \sum_{n=1}^{N} (\varepsilon_n - \varepsilon_0) L_n G(x_n, x') \mathrm{e}^{ik_0|x-x_n|}, \tag{26}$$

where $G_0(x, x') = \frac{\mathrm{e}^{ik_0|x-x'|}}{2ik_0}$ is the Green's function in a 1D medium without scatterers and L_n is the width of the scattering layer. The Green's function in the 2D case is

$$G(\mathbf{r}_\perp, \mathbf{r}'_\perp) = G_0(\mathbf{r}_\perp, \mathbf{r}'_\perp) + i\frac{\omega^2}{4c^2} \sum_{n=1}^{N} (\varepsilon_n - \varepsilon_0) G(\mathbf{r}_{\perp n}, \mathbf{r}'_\perp) \times S_n H_0^{(1)}(k_0|\mathbf{r}_\perp - \mathbf{r}_{\perp n}|), \tag{27}$$

where $G_0(\mathbf{r}_\perp, \mathbf{r}'_\perp) = \frac{1}{4i} H_0^{(1)}(k_0|\mathbf{r}_\perp - \mathbf{r}'_\perp|)$ is the Green's function in a 2D medium without scatterers, $\mathbf{r}_\perp = \{x, y\}$ is 2D radius vector, and S_n is the area of the scatterer. In accordance with formulas (1), (26) and (27) the LDOS in 1D and 2D cases, respectively are

$$\rho(x,\omega) = \frac{\sqrt{\varepsilon_0}}{\pi c} - \frac{\omega^2\sqrt{\varepsilon_0}}{\pi c^3}\sum_{n=1}^{N}(\varepsilon_n - \varepsilon_0)L_n \times \mathrm{Im}[iG(x_n,x)\mathrm{e}^{ik_0|x-x_n|}], \tag{28}$$

$$\rho(\mathbf{r}_\perp,\omega) = \frac{\omega\varepsilon_0}{2\pi c^2} - \frac{\omega^3\varepsilon_0}{2\pi c^4}\sum_{n=1}^{N}(\varepsilon_n - \varepsilon_0)S_n \times \mathrm{Im}[iG(\mathbf{r}_{\perp n},\mathbf{r}_\perp)H_0^{(1)}(k_0|\mathbf{r}_\perp - \mathbf{r}_{\perp n}|)]. \tag{29}$$

The first terms in formulas (28) and (29) represent the LDOS in the host media and the second terms are contributions due to the presence of scatterers. For identical scatterers formulas (18), (28), and (29) give

$$\rho(x,\omega) = \frac{\sqrt{\varepsilon_0}}{\pi c} - \frac{\omega^2\sqrt{\varepsilon_0}L_1}{\pi c^3}(\varepsilon_1 - \varepsilon_0) \times \sum_{n=1}^{N}\mathrm{Im}[iG(x_n,x)\mathrm{e}^{ik_0|x-x_n|}], \tag{30}$$

$$\rho(\mathbf{r}_\perp,\omega) = \frac{\omega\varepsilon_0}{2\pi c^2} - \frac{\omega^3\varepsilon_0 S_1}{2\pi c^4}(\varepsilon_1 - \varepsilon_0) \times \sum_{n=1}^{N}\mathrm{Im}[iG(\mathbf{r}_{\perp n},\mathbf{r}_\perp)H_0^{(1)}(k_0|\mathbf{r}_\perp - \mathbf{r}_{\perp n}|)], \tag{31}$$

$$\rho(\mathbf{r},\omega) = \frac{\omega^2\varepsilon_0^{3/2}}{2\pi^2 c^3} - \frac{\omega^3\varepsilon_0 V_1}{2\pi^2 c^4}(\varepsilon_1 - \varepsilon_0) \times \sum_{n=1}^{N}\frac{\mathrm{Im}[G(\mathbf{r}_n,\mathbf{r})\mathrm{e}^{ik_0R_n}]}{R_n}. \tag{32}$$

The formulas (30)–(32) explicitly show that the LDOS depends on: frequency, number of scatterers and on contrast $\varepsilon_1 - \varepsilon_0$ and size L. Amplitude variations of the LDOS are proportional to the contrast and size of scatterers, and the LDOS decreases when distances between the particles grow. This shows that the influence of many closely spaced small particles on the LDOS can be essential even if their scattering parameters (contrast and size) are "weak".

3.3. Numerical examples

When the medium contains more than two particles, analytical calculation of the LDOS (and the Green's functions as well) becomes a tedious task and the problem should be treated numerically. Below we calculate the LDOS for typical 1–2D structures and compare them to results presented in the literature.

3.3.1. 1D medium

It will be instructive to calculate the transmission in 1D medium with layers by using LPM and compare it with the exact result obtained with the help of the transfer matrix theory [38]. The transmission T can be expressed in terms of the Green's function as (see Appendix B)

$$T(x) = \left|\frac{G(x,x')}{G_0(x,x')}\right|^2, \tag{33}$$

where $G(x,x')$ and $G_0(x,x')$ are the Green's functions of the medium with and without the layers. Note that the point source (placed at x') is placed before the structure and measurement point x is placed after the structure. We consider the structure consisting of eight cells formed by alternating layers with high ($\varepsilon_n = 2.56$) and low ($\varepsilon_0 = 1$) permittivity. The period of the structure is $d = 1$ μm, and the width of the layer with high permittivity (scattering layer) is $L = 0.25$ μm. Fig. 6 a shows the transmission T calculated with the help of LPM formulas (26) and (33) and by using the exact transfer matrix theory. The dashed curve shows transmission for the structure with $L = 0.25$ μm and the solid curve (coincided with marked one) shows transmission for the structure when each scattering layer was subdivided into five identical layers with $L_{\mathrm{sub}} = L/5 = 0.05$ μm. In the latter case the number of scatterers increased by 5, however the accuracy increased dramatically (see Fig. 6a). Fig. 6a shows that for layers with $L = 0.25$ μm there is an extremely good agreement between exact and calculated results until values $\omega d/2\pi c = k_0L/1.6 \sim 0.2$, which is an upper limit of the theory. Decreasing the width of the layers increases the accuracy for higher values $\omega d/2\pi c$. Fig. 6b presents the difference between exact and calculated transmissions versus $\omega d/2\pi c$, for $L = 0.25$ μm and $L_{\mathrm{sub}} = 0.05$ μm. Fig. 6b shows that in general discrepancies increase with $\omega d/2\pi c$ and especially toward the band edges, where T changes rapidly. Taking layers with $L_{\mathrm{sub}} = 0.05$ μm we increase accuracy of the calculation in 10 times.

Finally, we compare the LDOS presented in Ref. [19](Fig. 7a) and one calculated with the help of LPM (Fig. 7b) for the 1D stack. The structure consists of eight identical cells with alternating dielectric ($L = 0.25$ μm, $\varepsilon_n = 2.56$) and vacuum ($\varepsilon_0 = 1$) layers. The period of the stack is $d = 1$ μm. The LDOS was calculated by using $L_{\mathrm{sub}} = L/5$ at the central vacuum

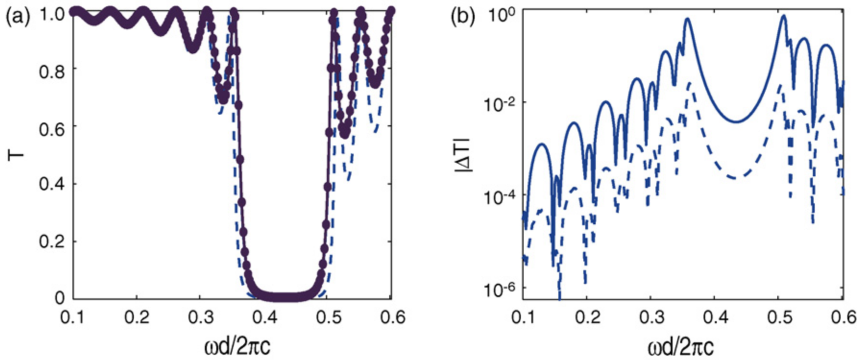

Fig. 6. (a) The exact and calculated with the help of our method (LPM) transmission T for 1D stack versus $\omega d/2\pi c$. The structure consists of eight cells with period $d = 1$ μm. Each cell is formed by dielectric layer with $L = 0.25$ μm, $\varepsilon_n = 2.56$ and vacuum layer with $\varepsilon_0 = 1$. The curve marked with dots shows exact transmission for the structure. The dashed curve shows transmission calculated for $L = 0.25$ μm. The solid curve (coinciding with marked one) shows transmission calculated when dielectric layer was subdivided into five layers with $L_{\text{sub}} = 0.05$ μm. (b) Modulus of difference $|\Delta T|$ (on logarithmic scale) between exact transmission and calculated one for structure with $L = 0.25$ μm (solid curve) and $L_{\text{sub}} = 0.05$ μm (dashed curve).

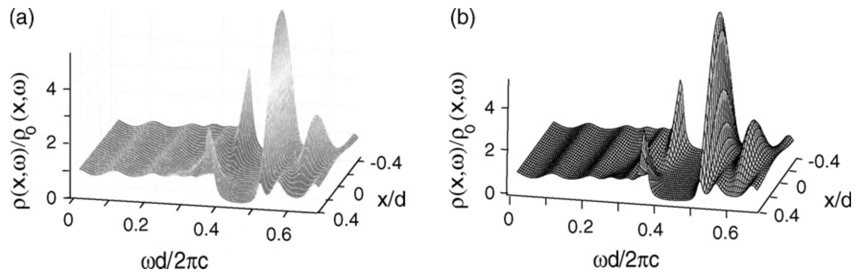

Fig. 7. (a) The LDOS presented in Ref. [19] for 1D stack versus $\omega d/2\pi c$ and position x/d. The structure consists of eight cells with period $d = 1$ μm. Each cell is formed by alternating dielectric layer with $L = 0.25$ μm, $\varepsilon_n = 2.56$ and vacuum layer ($\varepsilon_0 = 1$). The LDOS was calculated at the center of the stack, in vacuum layer. (b) Our results for the LDOS at the same stack versus $\omega d/2\pi c$ and position x/d inside the central vacuum layer.

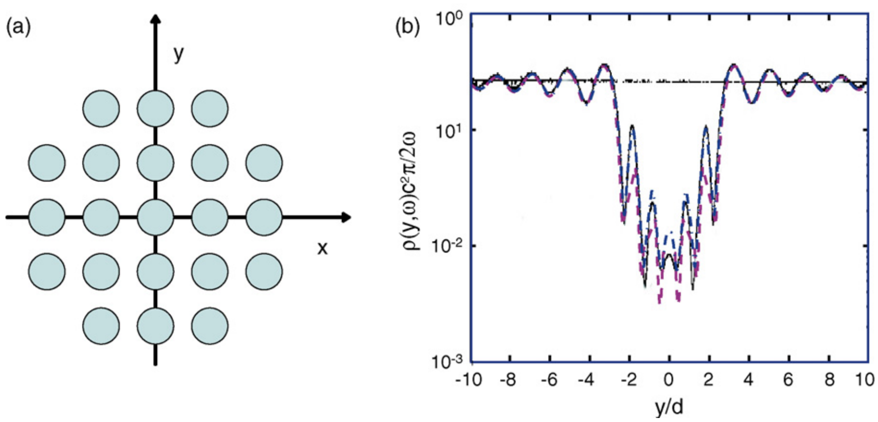

Fig. 8. (a) Configuration of cylinders. (b) The LDOS versus position y at $x = 0$ for array of dielectric cylinders. The solid line shows rigorous results calculated in Ref. [20], the dashed line shows our results for $L = 0.3d$, and the dash-dotted line represents our results for $L_{\text{sub}} = 0.3d/\sqrt{7}$. The parameters of the system are: $\lambda/d = 3.5$, $\varepsilon_n = 9$, and $\varepsilon_0 = 1$.

layer. One can see extremely good agreement between the results. Note that the number of frequency and coordinate points is 120 and 25, respectively. Time of calculation is 1.5 min.

3.3.2. 2D medium

For the 2D case we calculate the LDOS in array of dielectric cylinders (Fig. 8a) and compare our results with results obtained with the help of rigorous theory. Fig. 8b shows LDOS of the system calculated in Ref. [20] and our results. The array consists of 21 cylinders arranged in a square lattice formed by adding shells around the central cylinder. The parameters of the system are: period d, radius of the cylinders $L = 0.3d$, $\lambda/d = 3.5$, $\varepsilon_n = 9$, and $\varepsilon_0 = 1$. The LDOS is calculated as a function of y at $x = 0$. Fig. 8b shows that the LDOS calculated for $L = 0.3d$ (dashed line) reasonable agree with rigorous results despite the large value $k_0L = 0.54$ which is far from the validity limit ($k_0L \sim 0.1$) of the theory. Fig. 8b also shows the LDOS calculated for the case when each circle was subdivided into seven identical ones with radius $L_{\text{sub}} = 0.3d/\sqrt{7}$. One can see that in this case the accuracy of our results is increased. We used 250 coordinate points and calculation time was 12 s without subdivision and 13 min with subdivision. In order to obtain more accurate results we need to further increase subdivision, that would essentially increase the time of calculation.

4. Conclusions

In this paper we have studied numerically the local density of states (LDOS) in one-, two-, and three-dimensional finite size photonic structures. The LDOS has been calculated for vector and scalar fields with the help of the local perturbation method. It has been shown that the method provides accurate numerical tool for calculation of the LDOS in various photonic structures. The accuracy of calculation grows with increasing of computer memory.

Acknowledgments

We would like to thank W. Vos for assistance and critical comments, B. Husken and B. Kaas for helpful discussions. This work is part of the research program of the Stichting voor Fundamenteel Onderzoek der Materie, which is financially supported by the Nederlandse Organisatie voor Wetenschappelijk Onderzoek.

Appendix A. The calculation of the tensors $\{\hat{G}(\mathbf{r}_n, \mathbf{r}')\}$

Making first the differentiation in (10) and substituting after this $\mathbf{r}$ by $\mathbf{r}_n$, we obtain the following system of equations

$$\hat{G}(\mathbf{r}_n, \mathbf{r}') = \hat{G}_0(\mathbf{r}_n, \mathbf{r}') - \frac{\omega^2}{c^2}\sum_{n=1}^{N}(\varepsilon_n - \varepsilon_0)\hat{G}(\mathbf{r}_n, \mathbf{r}') \times \int_{-\infty}^{\infty}\int_{-\infty}^{\infty}\int_{-\infty}^{\infty}\left(\hat{I} - \frac{\mathbf{q}\otimes\mathbf{q}}{k_0^2}\right)\frac{f_n(\mathbf{q})}{(k_0^2 - q^2)}\,\mathrm{d}\mathbf{q}. \tag{A.1}$$

The system of Eq. (A.1) is linear with respect to $\hat{G}(\mathbf{r}_n, \mathbf{r}')$ and can be easily solved. The integrals in (A.1) can be calculated analytically or numerically for different particles (at least for sphere and cube). Note that dimensions of the particles implicitly present in the functions $f_n(\mathbf{q})$. Additional information about such calculations one can find also in the appendix of work [30].

Appendix B. The transmission of one-dimensional structure in one-dimensional case

Consider transmission of one-dimensional structure in one-dimensional case. Suppose that source of the incident field E_0 is a point source placed at point x' before the structure. The field E is the field after the structure. In this case the transmission T of the structure at point x is

$$T = \left|\frac{E(x)}{E_0(x)}\right|^2 = \left|\frac{\int_{-\infty}^{\infty} G(x,x'')\delta(x'-x'')\,\mathrm{d}x''}{\int_{-\infty}^{\infty} G_0(x,x'')\delta(x'-x'')\,\mathrm{d}x''}\right|^2 = \left|\frac{G(x,x')}{G_0(x,x')}\right|^2, \tag{B.1}$$

where $G(x, x')$ is the Green's function of the medium with the structure and $G_0(x, x')$ is the free-space Green's function.

References

[1] J. Rarity, C. Weisbuch (Eds.), Microcavities and Photonic Bandgaps: Physics and Applications, Kluwer Academic, New York, 1996.
[2] W.J. Wadsworth, et al. J. Opt. Soc. Am. B 19 (2002) 2148.
[3] V. Prosentsov, et al. Proc. SPIE 4974 (2003) 193.
[4] S. Noda, T. Baba (Eds.), Roadmap on Photonic Crystals, Kluwer Academic, New York, 2003.
[5] P. Lodahl, et al. Nature 430 (2004) 654.
[6] E.M. Purcell, Phys. Rev. 69 (1946) 681.
[7] E. Merzbacher, Quantum Mechanics, third ed., Wiley, 1998.

[8] S.M. Barnett, et al. J. Phys. B 29 (1996) 3763.
[9] V. Weisskopf, E. Wigner, Z. Phys. 63 (1930) 54.
[10] P. Bykov, Sov. J. Quantum Electron. 4 (1975) 861.
[11] M. Lewenstein, et al. J. Phys. B 21 (1988) L9.
[12] E.N. Economou, A. Zdetsis, Phys. Rev. B 40 (1989) R1334.
[13] S. Satpathy, Z. Zhang, M.R. Salehpour, Phys. Rev. Lett. 64 (1990) 1239.
[14] R. Sprik, B.A. Tiggelen, A. Lagendijk, Europhys. Lett. 35 (1996) 265.
[15] K. Busch, S. John, Phys. Rev. E 58 (1998) 3896.
[16] A. Moroz, Europhys. Lett. 46 (1999) 419.
[17] Z.Y. Li, Y. Xia, Phys. Rev. A 63 (2001) 43817.
[18] G. Boedecker, C. Henkel, Opt. Express 11 (2003) 1590.
[19] G. Boedecker, et al., in: Photonic Crystals, K. Busch, et al. (Eds.), Wiley, Weinheim, 2004.
[20] A.A. Asatryan, et al. Phys. Rev. E 63 (2001) 46612.
[21] A.A. Asatryan, et al. Waves Random Media 13 (2003) 9.
[22] G. Tayeb, D. Maystre, J. Opt. Soc. Am. A 14 (1997) 3323.
[23] M. Wubs, A. Lagendijk, Phys. Rev. E 65 (2002) 46612.
[24] D.P. Fussell, R.C. McPhedran, C. Martijn de Sterke, Phys. Rev. E 70 (2004) 46612.
[25] C. Hermann, O. Hess, J. Opt. Soc. Am. B 19 (2002) 3013.
[26] S. Kole, Ph.D. Thesis, University of Groningen, 2003.
[27] T.O. Korner, W. Fichtner, Techn. Proceeding of the 1998 International Conference on Modeling and Simulation of Microsystems, vol. 339 , 2005.
[28] A. Taflove, S.C. Hagness, Computational Electrodynamics: The Finite-Difference Time-Domain Method, third ed., Artech House Publ., 2005.
[29] O.J.F. Martin, C. Girard, A. Dereux, Phys. Rev. Lett. 74 (1995) 526.
[30] P.C. Chaumet, A. Sentenac, A. Rahmani, Phys. Rev. E 70 (2004) 36606.
[31] O.J.F. Martin, et al. Phys. Rev. Lett. 82 (1999) 315.
[32] F.G. Bass, V.D. Freilikher, V.V. Prosentsov, J. Electromagnet. Waves Appl. 14 (2000) 269.
[33] M. Lax, Phys. Rev. 94 (1954) 1391.
[34] I.M. Lifshits, Nuovo Cimento 3 (Suppl.) (1956) 716.
[35] A.A. Maradudin, Theoretical and Computational Aspects of the Effects of Point Defects and Disorder on the Vibrations of Crystals, Academic Press, New York, 1966.
[36] P. de Vries, D.V. van Coevorden, A. Lagendijk, Rev. Mod. Phys. 70 (1998) 447.
[37] D.S. Jones, Acoustic and Electromagnetic Waves, Clarendon Press, Oxford, 1986, p. 441.
[38] M. Born, E. Wolf, Principles of Optics, seventh ed., Cambridge University Press, Cambridge, 1999.